Cell Metabolism, Volume *14*

Supplemental Information

Heterozygosity for a Loss-of-Function Mutation in *GALNT2* Improves Plasma Triglyceride Clearance in Man

Adriaan G. Holleboom, Helen Karlsson, Ruei-Shiuan Lin, Thomas M. Beres, Jeroen A. Sierts, Daniel S. Herman, Erik S.G. Stroes, Johannes M. Aerts, John J.P. Kastelein, Mohammad M. Motazacker, Geesje M. Dallinga-Thie, Johannes H.M. Levels, Aeilko H. Zwinderman, Jonathan G. Seidman, Christine E. Seidman, Stefan Ljunggren, Dirk J. Lefeber, Eva Morava, Ron A. Wevers, Timothy A. Fritz, Lawrence A. Tabak, Mats Lindahl, G. Kees Hovingh, and Jan Albert Kuivenhoven

INVENTORY OF SUPPLEMENTAL INFORMATION

1. **Figure S1**. Figure not directly related to a figure of the main text. It illustrates that *GALNT2* mRNA and protein are not different in fibroblasts cultured from skin biopsies of three carriers of the mutation and three unrelated controls.

2. **Figure S2**. Figure 2 of the main text shows changes in plasma triglyceride levels over time in carriers and non-carriers after receiving an oral fat load. Supplemental figure 2 provides information on the distribution of apoC-III over lipoproteins and changes in cholesterol and triglyceride contents of the main lipoprotein fractions before (t=0) and after an oral lipid load (t=4).

3. **Figure S3.** Figure not directly related to a figure of the main text. It provides a 3-dimensional model of the domain in which the p.D314A mutation is located.

4. **Figure S4.** Figure not directly related to a figure of the main text. It provides information on putative substrates for ppGalNAc-T2.

5. **Table S1**. Table not directly related to a table of the main text. It shows evolutionary conservation of an asparagine residue at position 314 of ppGalNAc-T2

6. **Table S2**. Table related to table 1 of the main text. It provides individual lipid data of family members of the two index cases in which the p.D314A defect was identified.

7. **Table S3**. The table provides the outcome of mass spectrometry analyses of the apoC-III isoforms shown in figure 1 of the main text.

8. **Movie S1.** Shows the location of D314 and the hydrogen bond it forms with the amide nitrogen of Y317

Figure S1

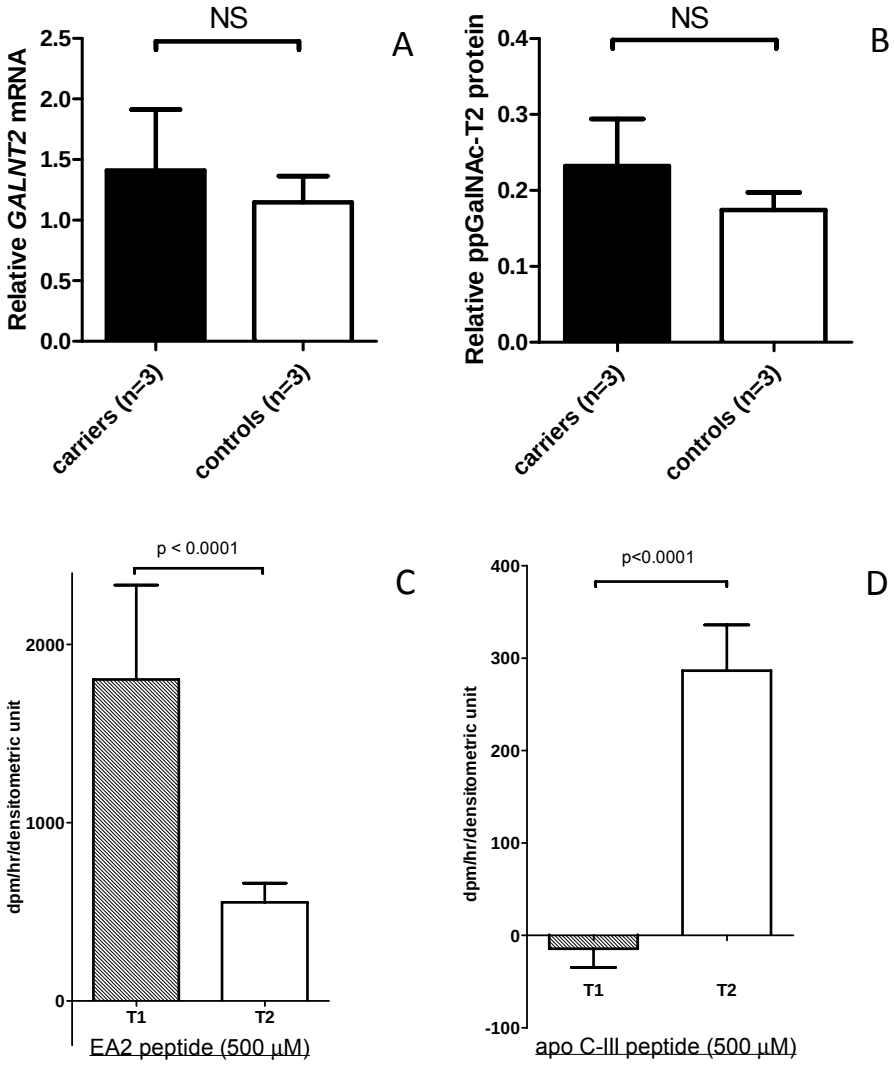
NS
A
Relative GALNT2 mRNA
2.5
2.0
1.5
1.0
0.5
0.0
carriers (n=3)
controls (n=3)
NS
B
Relative ppGalNAc-T2 protein
0.4
0.3
0.2
0.1
0.0
carriers (n=3)
controls (n=3)
p < 0.0001
C
dpm/hr/densitometric unit
2000
1000
0
T1
T2
EA2 peptide (500 µM)
p<0.0001
D
dpm/hr/densitometric unit
400
300
200
100
0
-100
T1
T2
apo C-III peptide (500 µM)

Figure S2

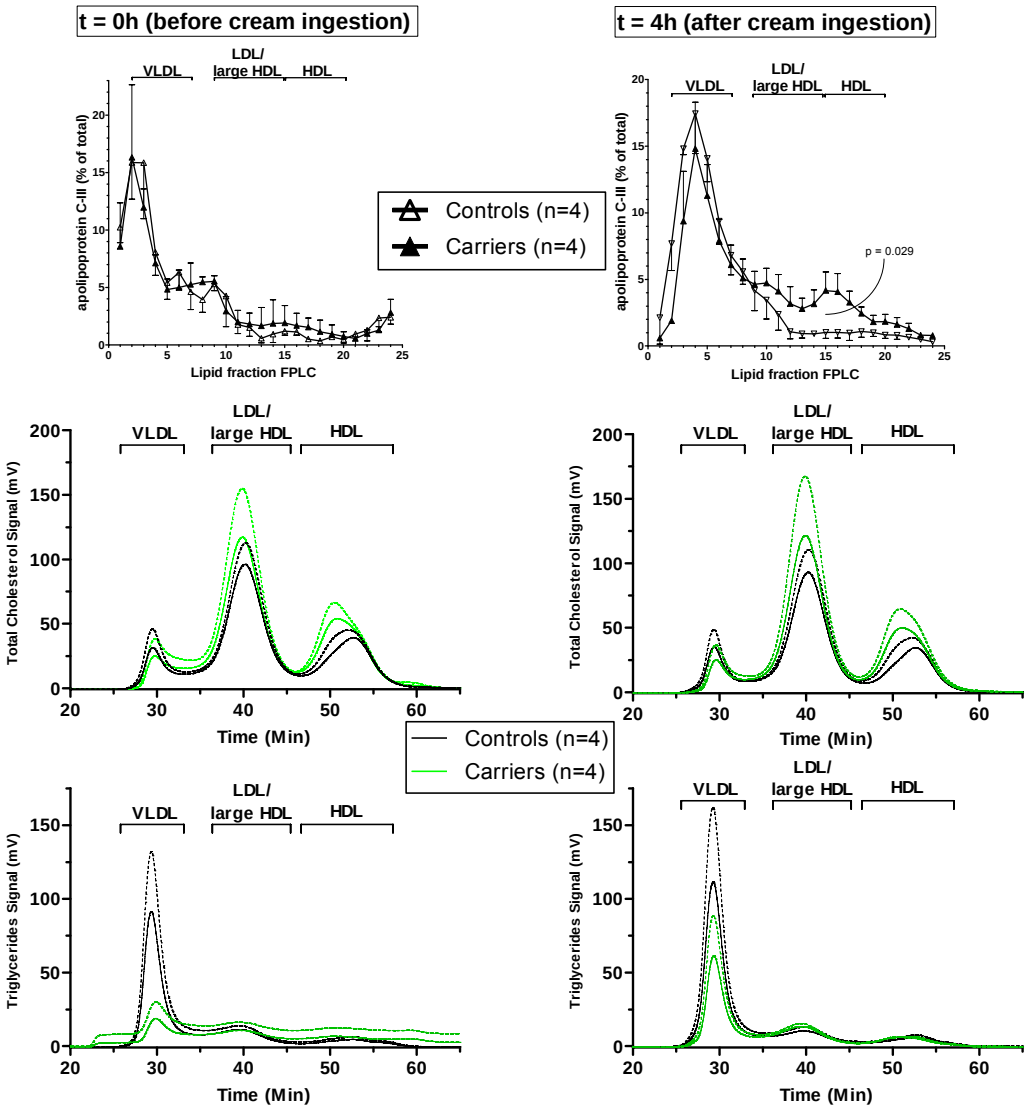
t = 0h (before cream ingestion)
t = 4h (after cream ingestion)
VLDL
LDL/ large HDL
HDL
apolipoprotein C-III (% of total)
Lipid fraction FPLC
Controls (n=4)
Carriers (n=4)
p = 0.029
Total Cholesterol Signal (mV)
Triglycerides Signal (mV)
Time (Min)

Figure S3

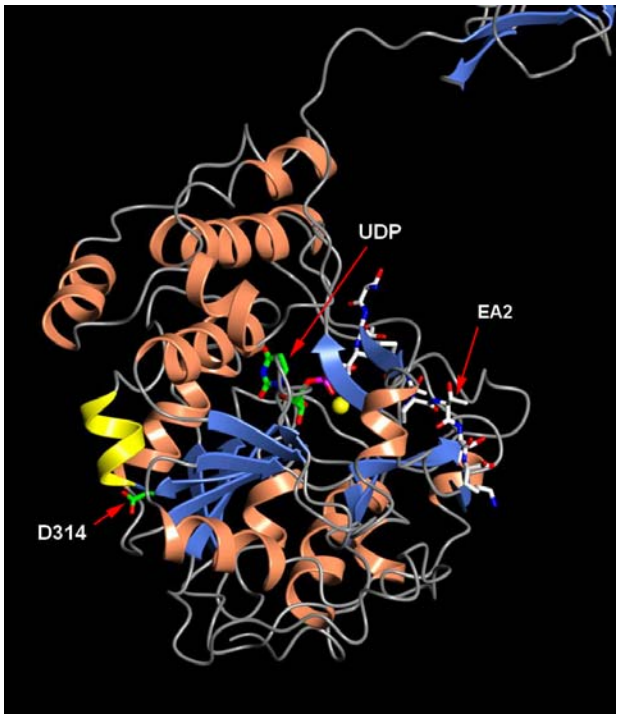

Figure S4

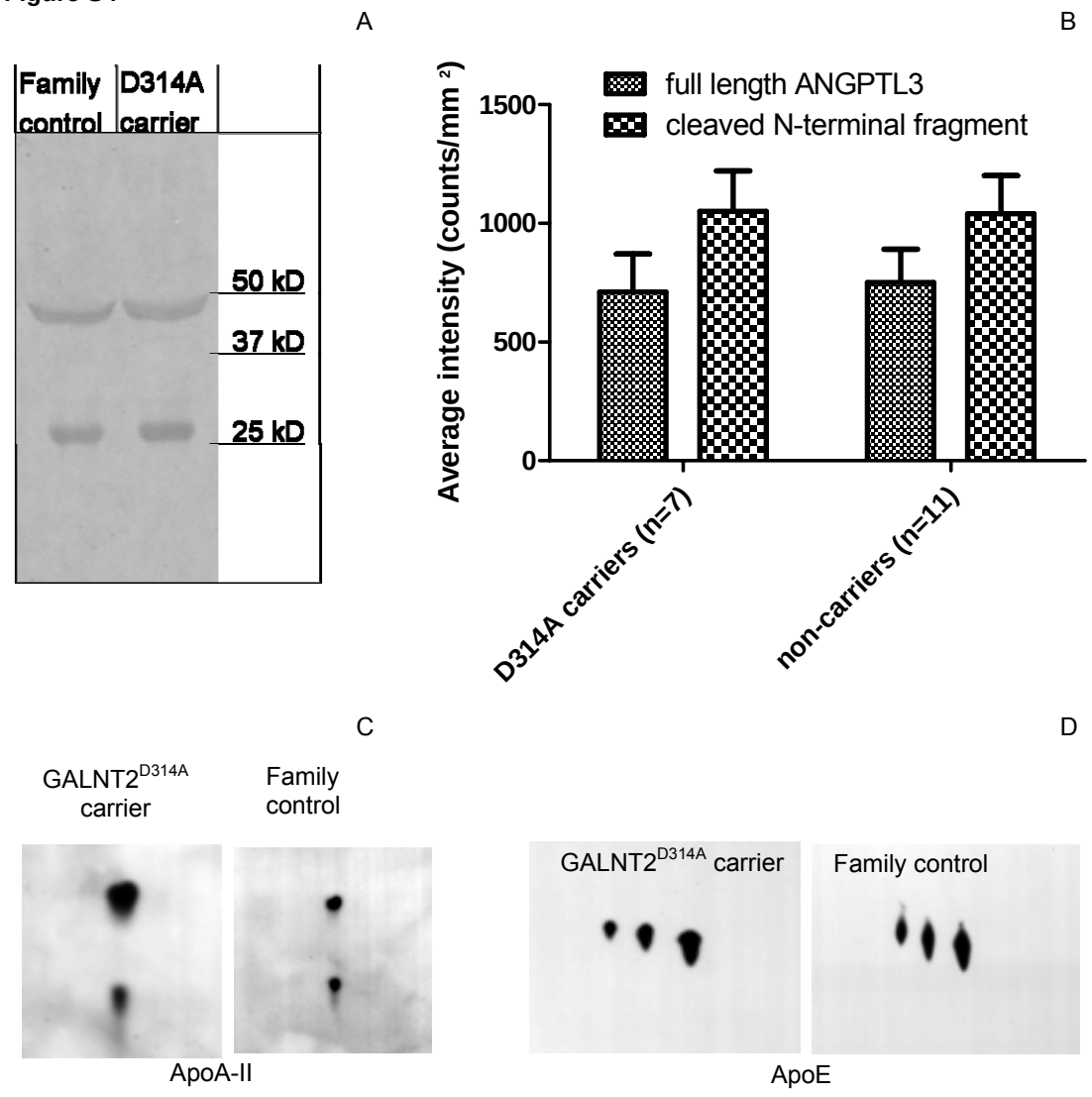
A
B
Family control
D314A carrier
50 kD
37 kD
25 kD
full length ANGPTL3
cleaved N-terminal fragment
Average intensity (counts/mm ²)
1500
1000
500
0
D314A carriers (n=7)
non-carriers (n=11)
C
D
GALNT2D314A carrier
Family control
ApoA-II
GALNT2D314A carrier
Family control
ApoE

LEGENDS TO FIGURES

Figure S1. Panels A and B show the effect of the *GALNT2* mutation on mRNA and protein levels. Panels C and D show O-linked glycosylation of peptide substrates by ppGalNAc-T1 and ppGalNAc-T2. Panel ***A*** shows that *GALNT2* mRNA levels as assessed by qPCR in lysates of skin fibroblast cultures of three *GALNT2*^{D314A} carriers are not different from those of three unrelated controls, p for Mann Whitney U test: 0.48. *GALNT2* expression data were normalized for 36B4 housekeeping gene expression. Panel ***B*** shows ppGalNAc-T2 protein levels in lysates of the same cultured fibroblasts (quantified using Western analyses). Protein levels normalized for β-actin are similar in carriers and controls, p for Mann-Whitney-U = 0.72. The bars indicate means, and the whiskers standard deviations. Panels ***C*** and ***D*** show O-linked glycosylation of EA2 and an 11-mer apoC-III peptide with human ppGalNAc-T1 and ppGalNAc-T2. Vertical axis indicates rate of transfer as dpm/h/densitometric unit of enzyme. The different ppGalNAc transferases were overexpressed in COS7 cells. Panel ***C*** shows that the EA2 peptide, a standard ppGalNAc-T substrate, is a substrate for ppGalNAc-T1 (T1, grey bar) and for ppGalNAc-T2 (T2, white bar) but that ppGalNAc-T1 has a significantly higher activity (p for Student's t-test <0.0001). Panel ***D***: In contrast, ppGalNAc-T1 exhibited no catalytic activity towards an 11-mer apoC-III substrate (p for Student's t-test: <0.0001 compared to ppGalNAc-T2 activity). Reactions lacking peptide yielded background values that were averaged for each isoform and subtracted from each value obtained using either substrate. Adjusted values were averaged to give values shown. Error bars indicate SDs. The data are obtained through 3 independent experiments that were each carried out in triplicate.

Figure S2. Distribution of apoC-III over lipoprotein fractions during oral fat challenge. Average total apoC-III levels were not different between carriers and controls at both time points (t=0h: 8.7 (SD 1.8), versus 10 (SD 0.41), ns using MW-U), and at t=4h: 8.5 (SD 2.0), versus 9.1 (SD 1.0), ns using MW-U). The upper two panels represent FPLC fractionated plasma that was used for apoC-III immunoblotting. Prior to ingestion of the cream upper left (top panel), apoC-III was similarly distributed over the lipoproteins in 4 carriers of the p.D314A-mutation (closed symbols) and the 4 non-carriers (open symbols). 4 hours after cream ingestion, however, the percentage of total apolipoprotein C-III in the HDL fraction was significantly increased in carriers compared to controls (upper right panel, average area under curve HDL fraction for carriers 23.4 (SD 6.0), for controls 8.2 (SD 2.6), p for MW-U = 0.029. Symbols represent means, whiskers represent SD. Lower four panels: FPLC cholesterol and triglyceride profiles obtained by inline cholesterol and triglyceride measurements of the eluent. The cholesterol profile shows that the HDL fraction is shifted to the left in the carriers compared to non-carriers which is indicative of larger HDL particle size. Only triglycerides in the VLDL-fraction tended to be lower in the carriers (p for MW-U of AUCs: 0.057) at t = 0h) compared to non-carriers. Continuous lines represent averages for 4 participants (green: carriers, lack: controls), dashed lines represent + 1 SD.

Figure S3. Molecular modelling of D314A mutation in ppGalNAc-T2. The figure shows a ribbon diagram of the human T2 structure (PDB ID 2ffu). Alpha helices (except as noted) are shown in

orange, beta strands in blue and loop regions in gray. Residue D314 (green carbons) is at the N-terminus of an alpha helix (yellow ribbon) which lies on the side of the catalytic domain opposite to that of the substrate binding face. The enzyme is shown with bound EA2 peptide (white carbons), UDP (green carbons) and a manganese ion (yellow sphere). A portion of the lectin domain is shown in the upper right of the figure. The figure was created using CCP4mg software (Potterton et al., 2004).

Figure S4. Other potential ppGalNAc-T2 substrates. Panel ***A*** shows a Western blot of plasma angiopoietin-related protein 3 of a p.D314A carrier and a non-carrier. In both samples full length (upper band) as well as processed angiopoietin-related protein 3 (lower band) can be discerned. Quantification of these signals did not reveal differences in full length angiopoietin-related protein 3 and the processed N-terminal fragment in 7 carriers and 11 non-carriers (Panel ***B***). Whiskers denote SDs. Panels ***C*** and ***D*** show 2-DE analyses of apoA-II and apoE isoforms in a carrier of the p.D314A mutation compared to a non-carrier. No detectable variation in isoform distribution of apoA-II (Expasy 2DE page ApoA-II, 2011) and apoE (Expasy 2DE page ApoE, 2010) was found after Western Blotting.

Table S1

Homo sapiens D314A	..TPMIAGGLFVM ***A*** KFYFEELGKYDMMMDVWGGE..
Homo sapiens	..TPMIAGGLFVM **D** KFYFEELGKYDMMMDVWGGE..
Rhesus	..TPMIAGGLFVM **D** KFYFEELGKYDMMMDVWGGE..
Mouse	..TPMIAGGLFVM **D** KLYFEELGKYDMMMDVWGGE..
Dog	..TPMIAGGLFVM **D** KLYFEELGKYDMMMDVWGGE..
Elephant	..TPMIAGGLFVM **D** KSYFEELGKYDMMMDVWGGE..
Opossum	..TPMIAGGLFVM **D** KFYFEELGKYDMMMDVWGGE..
Chicken	..TPMIAGGLFVM **D** KSYFEELGKYDMMMDVWGGE..
Xenopus tropicalis	..TPMIAGGLFVI **D** KSWFNQLGKYDTQMDIWGGE..
Zebrafish	..TPMIAGGLFVM **D** KDYFEELGKYDMMMDVWGGE..
Fruitfly	..TPMIAGGLFVI **D** KAYFNKLGKYDMKMDVWGGE..

Table S2

	Sex	Total cholesterol (mg/dl)	HDL-cholesterol (mg/dl)	LDL-cholesterol (mg/dl)	Triglycerides (mg/dl)
Carrier 1 (I-5, proband of 1st family)	M	251	90	148	72
Carrier 2 (I-1, proband of 2nd family)	F	305	121	168	93
Average and SD		*278 (38)*	*106 (21)*	*158 (14)*	*82.4*[†]
P (vs. controls)		*<0.01*	*<0.0001*	*0.27*	*0.35*[§]
Carrier 3 (I-2)	M	266	64	200	115
Carrier 4 (I-6)	F	176	62	101	62
Carrier 5 (II-6)	F	287	82	181	73
Carrier 6 (II-8)	F	288	59	179	94
Carrier 7 (II-9)	F	240	66	150	45
Carrier 8 (III-1)	F	192	47	125	86
Average and SD		*242 (48)*	*63 (11)*	*156 (38)*	*80 (59-100)*[†]
P (vs. controls)		*0.026*	*0.20*	*0.12*	*0.064*[§]
All carriers					
Average and SD	*N/A*	*251 (46)*	*74 (23)*	*157 (32)*	*80 (65-94)*[†]
P (vs. controls)		*0.004*	*0.017*	*0.070*	*0.05*[§]
Family control 1 (I-1)	F	185	61	129	93
Family control 2 (I-3)	F	137	63	78	83
Family control 3 (I-4)	F	269	53	191	98
Family control 4 (I-7)	M	215	57	160	90
Family control 5[‡]	M	170	*64*	101	*55*
Family control 6 (II-1)	M	158	41	101	117
Family control 7 (II-2)	M	205	44	137	117
Family control 8 (II-3)	F	202	42	135	134
Family control 9 (II-4)	M	215	46	172	110
Family control 10 (II-5)	M	194	52	144	75
Family control 11 (II-7)	F	111	61	55	85
Family control 12 (II-10)	M	220	46	176	173
Family control 13 (II-11)	M	245	75	147	135
Family control 14 (II-12)	F	207	45	140	76
Family control 15 (2nd family, II-1)	F	220	83	107	87
Family control 16 (2nd family, II-2)	F	191	63	109	155
Family control 17 (2nd family, II-3)	M	174	57	91	91
All controls					
Average and SD		*195 (38)*	*56 (12)*	*128 (37)*	*93 (72-114)*[†]

Table S3

ApoC-III isoforms	p*I*/Mass (Da)	Peptide Masses (Da)	Amino acid positions and corresponding sequences	Sequence coverage (%)
ApoC-III_2	4.2/10 000	898.42	52-58, DYWSTVK	34
		1196.61	41-51, GWVTDGFSSLK	
		1716.91	25-40, DALSSVQESQVAQQAR	
ApoC-III_1	4.4/8 900	898.43	52-58, DYWSTVK	34
		1196.61	41-51, GWVTDGFSSLK	
		1716.87	25-40, DALSSVQESQVAQQAR	
ApoC-III_0	4.6/8 900	898.40	52-58, DYWSTVK	34
		1196.59	41-51, GWVTDGFSSLK	
		1716.88	25-40, DALSSVQESQVAQQAR	
ApoC-III_0	4.6/8 800	1141.50	52-60, DYWSTVKDK	61
		1196.58	41-51, GWVTDGFSSLK	
		1716.92	25-40, DALSSVQESQVAQQAR	
		2137.03	61-79, FSEFWDLDPEVRP**T**SAVAA	
		2380.16	59-79, DKFSEFWDLDPEVRP**T**SAVAA	

LEGENDS TO TABLES

Table S1. Evolutionary conservation of an aspartic acid residue at position 314 of ppGalNAc-T2

Table S2. Individual lipid and lipoproteins of all family members.
Abbreviations: M, male; F, female; SD, standard deviation, N/A not applicable. Symbols: †, medians and interquartile ranges are given. For the 2 probands, no interquartile range can be given; ‡, son of grand nephew of proband not indicated in pedigree; §, triglycerides were log-transformed prior to comparison of means by T-test. P values were obtained with Student's T test.

Table S3. Characterization of apoC-III isoforms in HDL of a carrier of the *GALNT2*^{D314A} mutation with peptide mass fingerprinting using 2-E and MALDI-TOF mass spectrometry. The apoC-III isoforms (accession no. P02656) correspond to the di-sialylated (C-III_2), mono-sialylated (C-III_1) and non-sialylated (C-III_0, 8.8 and 8.9 kDa) variant as shown in figure 1 (Bruneel et al., 2007). Bold and underlined T indicates residue threonine 74 which carries the O-glycan chain.

LEGEND TO MOVIE

Movie S1. Movie showing the location of D314 and the hydrogen bond it forms with the amide nitrogen of Y317. ppGalNAc-T2 (PDB ID 2ffu) is shown as a ribbon diagram with orange alpha helices, blue beta strands and gray loops. The enzyme is bound to EA2 peptide (white carbons), UDP (green carbons) and a manganese ion (yellow sphere). The active site initially faces forward and the view of the enzyme then rotates 180 degrees to the side containing D314 (green carbons) and the alpha helix (yellow ribbon) to which D314 forms a hydrogen bond. A close up view shows the hydrogen bond (dashed blue line) between the D314 side chain and the amide nitrogen of Y317. The movie was created using CCP4mg software (Potterton et al., 2004).

SUPPLEMENTAL EXPERIMENTAL PROCEDURES

GALNT2 qPCR and ppGalNAc-T2 western blot of fibroblast lysates

mRNA was isolated from cultured fibroblasts (obtained by skin biopsies from the forearm) using Trizol (Invitrogen) and cDNA was prepared using Superscript II reverse transcriptase (Invitrogen). QPCR was performed on a MyiQ (Biorad) using primers for *GALNT2* (sequences available upon request) and for 36B4 as control. ppGalNAc-T2 protein was assessed in fibroblast lysates by standard western blotting techniques using anti-human ppGalNAc-T2 (Sigma no. HPA-011222) as primary antibody. Peptides were visualized using Licor Odyssey InfraRed detection system.

Two dimensional gel electrophoresis and Western blotting

Aliquots (5ul) of EDTA plasma from carriers (n=7) and controls (n=7) were used for 2-DE/Western blot analysis. Prior to 2-DE the protein concentrations were determined (Bradford, 1976) and the samples were dissolved in 0.25 ml sample solution according to Görg.(Gorg et al., 2000) 2-DE was performed using IPGphor and Multiphor (Amersham Biosciences) as described previously.(Karlsson et al., 2005) Shortly, proteins (300ug) for identification were separated on 3-10 IPGs and prior to Western blot samples containing 200ug of plasma protein were applied to pH 4-7 IPGs by in-gel rehydration for 12 h using low voltage (30 V). The proteins were then focused at 53 000 Vh at maximum voltage of 8000 V. The second dimension (SDS-PAGE) was performed by transferring the proteins to a homogenous (T=14%, C=1.5%) home-cast gel on gel bond running at 40–800 V, at 10 °C, 20–40 mA overnight. Proteins for identification were detected by silver staining (Shevchenko and Shevchenko, 2001) and images were evaluated by spot detection and intensities using a CCD camera and a Fluor-S Multi-imager in combination with a computerised imaging 12-bit system, PDQuest V8.0.1. (Bio-Rad).

In Western blots, proteins were transferred to a PVDF membrane in a trans-blot cell system (Bio-Rad) running for 2 h, 60V, 400 mA, in transfer buffer at pH 8.3. The membranes were blocked for 1 h in blocking buffer (5% non-fat dry milk/TBS pH 7.5), then washed in TTBS pH 7.5 and incubated in 2% non-fat milk in TTBS with primary antibodies overnight. Primary antibodies used were rabbit polyclonal anti–human apoC-III (Abcam, No. 21032; 1:5000), rabbit polyclonal anti-human apoA-II (Abcam, No. 24241; 1:5000) or goat polyclonal anti-human apoE (GenWay, No. 18272197662; 1:5000). After another wash in TTBS the membrane was incubated in 2% non-fat milk in TTBS with HRP conjugated secondary antibodies against goat, rabbit and mouse IgG (Bio Rad;1:40 000), respectively, for one hour. Proteins were visualized using the ECL plus western blotting detection system, exposed to X-ray film and developed. Isoform intensities were determined as optical density*mm2 (ODU) and expressed as % of the total protein level for each protein.

Mass spectrometry

Proteins from silver stained gels prepared as described abov were excised from the gel with a syringe and transferred to small Eppendorf tubes (0.5 mL). The gel pieces were washed twice with 50% acetonitrile/25 mM ammonium bicarbonate, with 100% acetonitrile once and dried in a SpeedVac vacuum concentration system (Savant, Farmingdale, NY, USA). About 0.25 mL of trypsin, (20 mg/mL in 25 mM ammonium bicarbonate) was added to the gel piece and the sample was incubated

overnight at 37°C. The supernatant was transferred to a separate tube and the peptides were further extracted from the gel piece by incubation in 50% acetonitrile/5% TFA for 5 h in room temperature. The supernatants from the two steps were then pooled, dried in SpeedVac and dissolved in 5ul 0.1% TFA. Peptides obtained after tryptic digestion were mixed 1:1 with a matrix (DHB, 0.02 mg/mL) in 70% acetonitrile/0.3% TFA, and then spotted on a stainless steel target plate. Analyses of peptide masses were performed using MALDI-TOF MS (Voyager DE PRO; Applied Biosystems) equipped with a 337 nm N2 laser operated in reflector mode with delayed extraction. Instrument settings optimized for DHB as described previously (Ghafouri et al., 2007) and positive ionization, delay time of 170 ns and accelerating voltage of 20 kV were used to collect spectra in the mass range 700–3600 Da. Data processing of spectra was performed in Data Explorer V4.0 (Applied Biosystems). External mass calibration with a standard peptide mixture and internal calibration using known trypsin autolysis peaks (m/z: 842.5100, 2211.1046) were also performed prior to the database search. Peptide masses (plus H+) with the greatest intensity (major peaks), in the spectra were submitted to database search. NCBI and Swiss-Prot were used with AIdente or MS-Fit as search engines. Restrictions were human species, mass tolerance 50 ppm, maximum one missed cleavage by trypsin and cysteine modification by carbamido-methylation.

Plasma fractionation

Plasma lipids were fractionated by fast performance liquid chromatography (Levels et al., 2003). ApoC-III in the fractions was quantified by spot blot with anti-human apoC-III as described above.

Desialylation of apoC-III

63 ug of apoC-III isolated from human VLDL (Academy Bio-Medical Company) was incubated with 60 mU neuraminidase (NorthStar) for 3 hours at 37°C in 50 mM sodium phosphate pH 5,0. As a control reaction the same amount of apoC-III was incubated without neuraminidase. 15 ug ApoC-III was incubated with human recombinant LPL for 2 hrs on ice prior to LPL activity measurement. LPL activity was measured as previously described (Nilsson-Ehle and Schotz, 1976).

Generation of secretion constructs

DNA constructs of wild-type human (h) T1, wild-type hT2, and mutant hT2 were generated using pKN55 (containing stem, catalytic, and lectin domains of human T1 (Fritz et al., 2004) and T2 (Fritz et al., 2006). Subcloning into pIMKF4 was performed using MluI and AgeI. The mutation changing the aspartic acid to an alanine at position 314 was created to replicate the naturally occurring mutation in hT2 using the Quikchange II XL Site Directed Mutagenesis Kit (Agilent Technologies) according to the manufacturer's protocol using pIMKF4-hT2 as a template and using the following primers:
5'- GTGGGCTGTTTGTGATGGCTAAGTTCTATTTTGAAGAAC-3' and 5'-
GTTCTTCAAAATAGAACTTAGCCATCACAAACAGCCCAC -3'.

O-linked glycosylation of EA2 and 11-mer apoC-III peptide with human ppGalNAc-T1 and ppGalNAc-T2

Abilities of EA2 and apoC-III peptides to act as in vitro substrates for wild-type ppGalNAcT-1 or ppGalNAcT-2 were compared using methods previously described. (Ten Hagen et al., 2003; Hagen et al., 1997) Briefly, each reaction (25 µl) contained 500 µM acceptor peptide substrate, 20 µM cold UDP-GalNAc, 0.4 µCi UDP-[1-^{14}C]GalNAc, 10 mM MnCl2, 0.1% Triton-X100, 40 mM 2-mercaptoethanol, 40 mM cacodylate (pH 6.5) Equivalent amounts of each FLAG-purified recombinant protein based on densitometry of FLAG immunoblots using ImageJ software were used in each reaction. The reaction mixture was incubated at 37 °C for 1 hr, stopped by addition of 20 µl of 150 mM EDTA, brought up to 100 µl, with deionized water and purified using AG 1-X8 anion exchanger (BioRad). The resin was washed 3 times with 100 µl of deionized water, and the flow-through was measured for radioactivity.

Angiopoietin-related protein 3 western blotting

Full length and processed angiopoietin-related protein 3 were assessed in plasma of carriers and non-carriers by standard western blotting techniques using anti-human angiopoietin-related protein 3 (R&D no. AF3829) as primary antibody. Peptides were visualized using Licor Odyssey InfraRed detection system (Westburg).

SUPPLEMENTAL REFERENCES

Bradford, M.M. (1976). A rapid and sensitive method for the quantitation of microgram quantities of protein utilizing the principle of protein-dye binding. Anal. Biochem. *72*, 248-254.

Bruneel, A., Robert, T., Lefeber, D.J., Benard, G., Loncle, E., Djedour, A., Durand, G., and Seta, N. (2007). Two-dimensional gel electrophoresis of apolipoprotein C-III and other serum glycoproteins for the combined screening of human congenital disorders of***O***- and***N***-glycosylation. PROTEOMICS - Clinical Applications *1*, 321-324.

Expasy 2DE page ApoA-II. 2011.
Ref Type: Online Source

Expasy 2DE page ApoE. http://www.expasy.org/swiss-2dpage/ac=P02649. 2010.
Ref Type: Online Source

Fritz, T.A., Hurley, J.H., Trinh, L.B., Shiloach, J., and Tabak, L.A. (2004). The beginnings of mucin biosynthesis: the crystal structure of UDP-GalNAc:polypeptide alpha-N-acetylgalactosaminyltransferase-T1. Proc. Natl. Acad. Sci. U. S. A *101*, 15307-15312.

Fritz, T.A., Raman, J., and Tabak, L.A. (2006). Dynamic association between the catalytic and lectin domains of human UDP-GalNAc:polypeptide alpha-N-acetylgalactosaminyltransferase-2. J Biol. Chem. *281*, 8613-8619.

Ghafouri, B., Karlsson, H., Mortstedt, H., Lewander, A., Tagesson, C., and Lindahl, M. (2007). 2,5-Dihydroxybenzoic acid instead of alpha-cyano-4-hydroxycinnamic acid as matrix in matrix-assisted laser desorption/ionization time-of-flight mass spectrometry for analyses of in-gel digests of silver-stained proteins. Anal. Biochem. *371*, 121-123.

Gorg, A., Obermaier, C., Boguth, G., Harder, A., Scheibe, B., Wildgruber, R., and Weiss, W. (2000). The current state of two-dimensional electrophoresis with immobilized pH gradients. Electrophoresis *21*, 1037-1053.

Hagen, F.K., Ten Hagen, K.G., Beres, T.M., Balys, M.M., VanWuyckhuyse, B.C., and Tabak, L.A. (1997). cDNA cloning and expression of a novel UDP-N-acetyl-D-galactosamine:polypeptide N-acetylgalactosaminyltransferase. J Biol. Chem. *272*, 13843-13848.

Karlsson, H., Leanderson, P., Tagesson, C., and Lindahl, M. (2005). Lipoproteomics II: mapping of proteins in high-density lipoprotein using two-dimensional gel electrophoresis and mass spectrometry. Proteomics. *5*, 1431-1445.

Levels, J.H., Lemaire, L.C., van den Ende, A.E., van Deventer, S.J., and van Lanschot, J.J. (2003). Lipid composition and lipopolysaccharide binding capacity of lipoproteins in plasma and lymph of patients with systemic inflammatory response syndrome and multiple organ failure. Crit Care Med. *31*, 1647-1653.

Nilsson-Ehle, P. and Schotz, M.C. (1976). A stable, radioactive substrate emulsion for assay of lipoprotein lipase. J. Lipid Res. *17*, 536-541.

Potterton, L., McNicholas, S., Krissinel, E., Gruber, J., Cowtan, K., Emsley, P., Murshudov, G.N., Cohen,S., Perrakis,A., and Noble,M. (2004). Developments in the CCP4 molecular-graphics project. Acta Crystallogr. D. Biol. Crystallogr. *60*, 2288-2294.

Shevchenko, A. and Shevchenko, A. (2001). Evaluation of the efficiency of in-gel digestion of proteins by peptide isotopic labeling and MALDI mass spectrometry. Anal. Biochem. *296*, 279-283.

Ten Hagen, K.G., Fritz, T.A., and Tabak, L.A. (2003). All in the family: the UDP-GalNAc:polypeptide N-acetylgalactosaminyltransferases. Glycobiology *13*, 1R-16R.